MORPHING LEADING-EDGE TUBERCLES ON CESSNA 172 WING

Giada Abate[1] & Hans Peter Monner[2]

[1]German Aerospace Center (DLR), Lilienthalplatz 7, 38108 Braunschweig, Germany, phone:+495312952439, email: giada.abate@dlr.de
[2]German Aerospace Center (DLR), Lilienthalplatz 7, 38108 Braunschweig, Germany

Abstract

Sinusoidal modifications of the leading-edge also called “tubercles” are applied to the Cessna 172 wing in order to study their aerodynamic effect. Originally, tubercles characterize the humpback whales’ flippers, and they help these giant animals to increase their speed and maneuverability into the water by acting like flow control devices. Studies showed that tubercles are similar to vortex generators and wing fences: they re-energize the leading-edge flow by generating vortices that can block most of the spanwise flow leading to a delay in flow separation and stall. It has been shown that they can successfully be applied to fans and wind turbine blades, but not many works highlight their positive effects on wing applications. Therefore, the present study wants to conduct an aerodynamic analysis of tubercles applied to the leading-edge of the Cessna 172 wing. A particular attention will be given to three design parameters: amplitude, wavelength, and wingspan location of tubercles. These variables characterize every single tubercle configuration, and their combination results in different aerodynamic flow effects. The aim of this analysis is to give some insights on tubercle parameterization and their geometric characteristics in order to achieve stall delay and relevant aerodynamic improvements in off-design regimes. Moreover, as mentioned before, since the positive effect of tubercles is only relevant at some flow conditions or regimes, the present work wants to consider the possibility of designing tubercles as morphing structures that are deployed only when needed by changing the shape of the leading-edge wing thanks to smart materials and actuators. Results show that only specific tubercle configurations give positive aerodynamic effects by increasing the lift-to drag ratio at high angles of attack.

Keywords: tubercles, Cessna 172, wing, morphing

1. Introduction

Tubercles are sinusoidal modifications characterizing the leading-edge of humpback whales’ flippers (Fig.1). They were discovered and studied for the first time by Fish and Battle [1], who highlighted how the presence of such sinusoidal modifications on the whales’ flippers allow these big animals to perform incredible turnings in the air. The physical principle behind them is still under investigation but according to the past studies, the idea is that such sinusoidal modifications act like vortex generators: they generate counter-rotating vortices that re-energize the boundary layer and delay flow separation [2, 3, 4, 5, 6]. Similarly, leading-edge bumps applied to wind turbine blades can increase the operative ranges of angle of attack and wind speed resulting in higher power production at high wind speeds [7, 8, 9, 10, 11, 12]. Another interesting finding was confirmed by Abate *et al.* [8, 9, 10, 11]. Tubercles not only act like vortex generators but they also have similarities with wing fences. According to this study, the vortices generated at the leading-edge by tubercles are able to block a portion of the spanwise flow at post-stall regimes. This positively affects the wind turbine blade aerodynamics leading to a stall delay and an improvement in the energy production at high wind speeds. Most of the past research on tubercles are experimental tests or computational fluid-dynamic analyses of leading-edge bumps on whale’s flipper models [2, 3, 4, 5, 6, 13, 14], wind turbine blades [7, 8, 9, 10, 11, 12], and infinite wings (airfoils) [15, 16, 17, 18, 19, 20, 21, 22, 23]. Just a few studies analyzed the three-dimensional effects of tubercles on aircraft wings, in particular on swept wings [24, 25, 26, 27, 28].

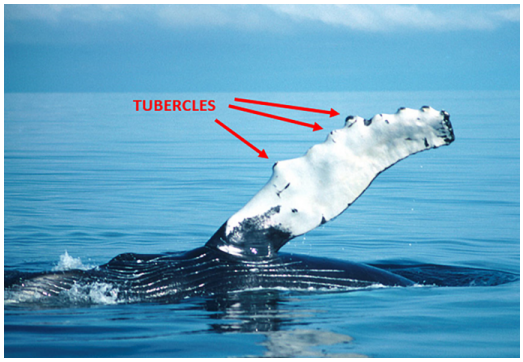

Figure 1 – Humpback whale flipper.[29]

Cross section airfoil	NACA 2412
Wing Span	11 m
Wing Area	16.2 m
Taper Ratio	0.672
Wing Root Chord	1.625 m
Wing Tip Chord	1.092 m
Sweep Angle	0 deg
Dihedral Angle	1.44 deg
Twist Angle	-3 deg

Table 1 – Cessna 172 Skyhawk specifications.

They concluded that tubercles affect the aerodynamics of swept wings by acting like vortex generators and wing fences leading to a flow separation delay. Moreover, tubercles enhance the lift coefficient in post-stall regime but most of the time, an increase in the drag coefficient was also visible. Most of these works are considering low Reynolds number values and they are not taking into account the effect of a variation in tubercle amplitude and wavelength.
The aim of the present study is to give some insights on tubercle characteristics (amplitude, wavelength, and span-coverage) for wing applications in order to achieve relevant aerodynamic improvements in off-design conditions. In addition, the concept explored in this study involves the consideration of morphing tubercles. This entails leveraging a combination of smart materials and actuators to enable the leading-edge of the wing to alter its shape into a sinusoidal configuration selectively, occurring only under specific flow conditions like high angles of attack.

2. Baseline Wing and Validation

It has been decided to choose the Cessna 172 Skyhawk as baseline wing because of its simplified geometry that could help the implementation of tubercles in both simulations and real testing. The general specifications of the Cessna 172 wing are listed in Tab.1, and its geometry is illustrated in Fig.2.
The baseline wing geometry has been reproduced in Ansys SpaceClaim©, and a computational fluid-dynamic (CFD) analysis has been conducted with Ansys Fluent©.
The fluid domain has a bullet shape as shown in Fig.3, and a box around the wing has been built in order to be able to refine the mesh only in that area (Fig.4). The mesh shown in Fig.5 is characterized by tetrahedral elements and 25 prism layers are close to the wing surface for a complete solution of the boundary layer. Therefore, the total number of mesh elements is about 18 millions.
For the CFD analysis, the flow is considered steady, compressible and fully turbulent with $k-\omega$ SST as turbulence model. As mentioned before, the boundary layer is completely solved considering a $y+<1$.
The boundary conditions are represented in Fig.6, the operative pressure is 101325 Pa, and the air speed is kept constant to 53.64 m/s which corresponds to the Cessna cruise speed. The flow angle

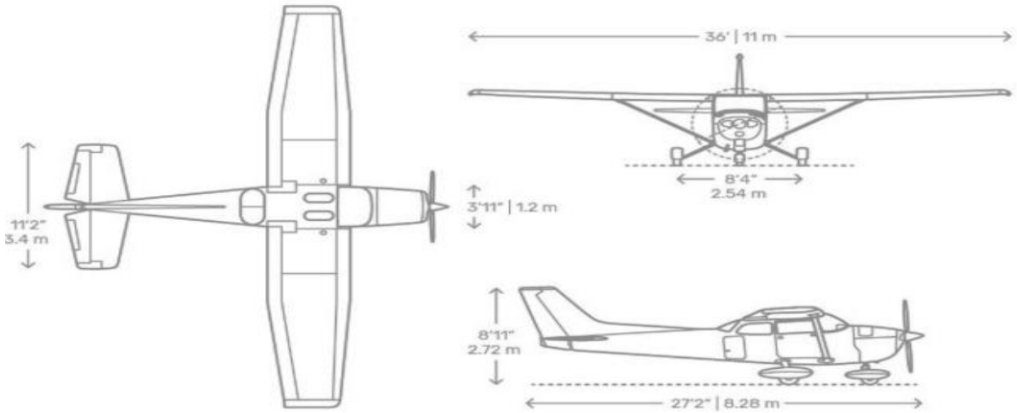

Figure 2 – Cessna 172 Skyhawk.[30]

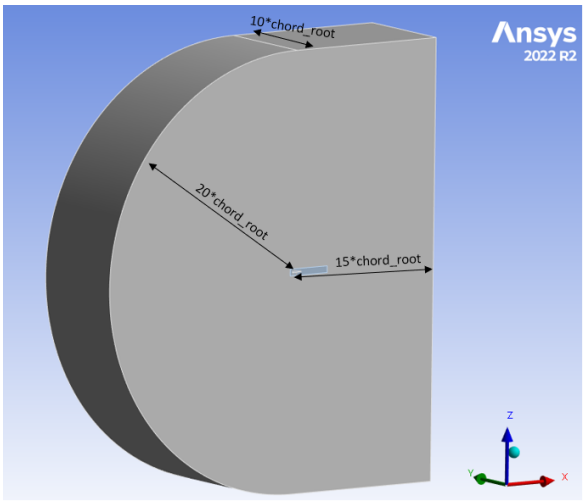

Figure 3 – CFD fluid domain.

of attack has been varied in order to plot the polar curve of the baseline wing to be compared with the experimental data coming from previous works [31, 32].
Several CFD simulations with an angle of attack between -2° and 18° have been run, and the results are shown in Fig.7. It is possible to notice that the polar curve coming from the CFD simulations is in accordance with previous and available experimental results [31, 32] conducted at two different air speeds: 33.18 m/s, and 20.48 m/s. From these results, it is possible to confirm that the baseline wing starts to stall at an angle of attack between 15.5° and 16°.

3. Cessna 172 Wing with Tubercles

3.1 Tubercle Parameterization

A parameterization of the wing geometry with tubercles has been conducted in order to simplify the generation of different tubercle configurations to be simulated. Tubercles are designed as sinusoidal leading-edge modifications characterized by an amplitude and a wavelength (Fig.8). Another important parameter to consider is the number of peaks that they identify. In this work, it has been decided to generate tubercles starting from the wing tip and covering only the second mid-span of the wing. Even though the Cessna wing starts to stall at the root, a previous sensitivity analysis showed that relevant aerodynamic effects of the sinusoidal leading-edge are visible only when it covers the wing from mid-span to the tip. Another important aspect to highlight is that tubercles can start and end either with a peak or a throat, this choice affects the aerodynamic results [11]. Therefore, in this work, tubercles start and end with the same cross-section meaning halfway between peak and throat.
Tubercles are generated by scaling the cross-section airfoil following a sinusoidal path and keeping

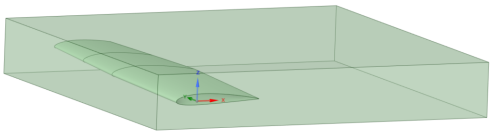

Figure 4 – Refinement box around the wing.

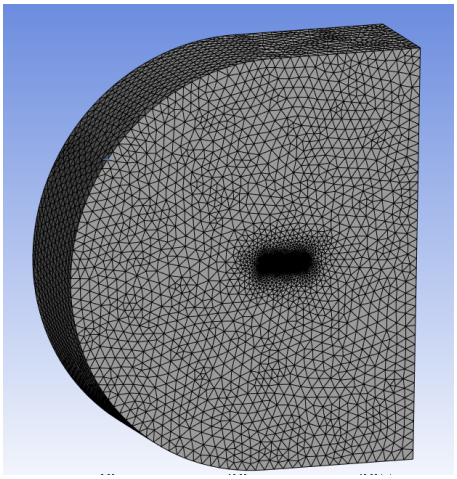

Figure 5 – CFD mesh.

fixed the trailing-edge line (Fig.9). Each airfoil chord varies by Δc, which is defined as:

$$\Delta c = A \sin\left(\frac{2\pi}{\lambda} y_{\text{tub}}\right) \tag{1}$$

where A is the amplitude, λ is the wavelength, and y_{tub} is the y-coordinate along the wingspan of each tubercle section. The new chord c at each airfoil section is then given by summing the original chord value (c_0) with the Δc previously calculated:

$$c = c_0 + \Delta c \tag{2}$$

For simplicity, non-dimensional values of amplitude and wavelength are considered:

$$\hat{A} = A / c_{\text{root}} \tag{3}$$

$$\hat{\lambda} = \lambda / l \tag{4}$$

where l is the mid-span length.

3.2 Design of Experiment

In order to explore the design space for the generation of the tubercle configurations to test, a design of experiment (DoE) has been considered. Amplitude, wavelength, and the number of tubercle peaks that cover the wing have been considered as three design variables. The resulting three-dimensional DoE explores the design space in order to find the region where specific values of the three design variables enhance the aerodynamic performance. In this study, amplitude and wavelength are treated as non-dimensional parameters. Additionally, the number of tubercle peaks is used to represent the proportion of the wing-span covered by tubercles. The ranges for non-dimensional amplitude and non-dimensional wavelength are 0.005-0.025 and 0.02-0.3, respectively. For the number of tubercles, the lower limit is 1 and the upper limit is defined considering a full coverage of the wing mid-span. Such value is strictly linked to the wavelength, and therefore, it is not unique for all the tubercle cases. Thirty tubercle configurations have been generated from the three-dimensional DoE, and the corresponding values of amplitude, wavelength and number of tubercle peaks are listed in Table 2.

	$\hat{A}$	A [m]	$\hat{\lambda}$	λ [m]	N.Peaks
Tb1	0.0050	0.0081	0.0200	0.055	1
Tb2	0.0150	0.0243	0.1600	0.440	4
Tb3	0.0200	0.0325	0.0900	0.247	4
Tb4	0.0100	0.0162	0.2300	0.632	3
Tb5	0.0125	0.0203	0.1250	0.343	5
Tb6	0.0225	0.0365	0.2650	0.728	1
Tb7	0.0175	0.0284	0.0550	0.151	16
Tb8	0.0075	0.0121	0.1950	0.536	3
Tb9	0.0087	0.0142	0.1075	0.295	9
Tb10	0.0187	0.0304	0.2475	0.680	2
Tb11	0.0237	0.0385	0.0375	0.103	19
Tb12	0.0137	0.0223	0.1775	0.488	2
Tb13	0.0112	0.0182	0.0725	0.199	5
Tb14	0.0212	0.0345	0.2125	0.584	4
Tb15	0.0162	0.0264	0.1425	0.391	1
Tb16	0.0062	0.0101	0.2825	0.776	3
Tb17	0.0068	0.0111	0.1512	0.415	4
Tb18	0.0168	0.0274	0.2912	0.800	3
Tb19	0.0218	0.0355	0.0812	0.223	3
Tb20	0.0118	0.0192	0.2212	0.608	4
Tb21	0.0143	0.0233	0.0462	0.127	19
Tb22	0.0243	0.0396	0.1862	0.512	2
Tb23	0.0193	0.0314	0.1162	0.319	6
Tb24	0.0093	0.0152	0.2562	0.704	1
Tb25	0.0081	0.0132	0.0637	0.175	9
Tb26	0.0181	0.0294	0.2037	0.560	1
Tb27	0.0231	0.0375	0.1337	0.367	6
Tb28	0.0131	0.0213	0.2737	0.752	2
Tb29	0.0106	0.0172	0.0987	0.271	2
Tb30	0.0206	0.0335	0.2387	0.656	3

Table 2 – Tubercle configurations.

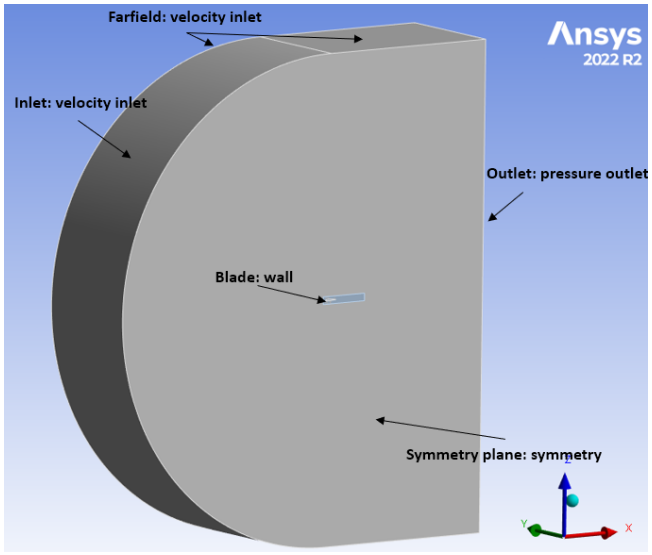

Figure 6 – CFD boundary conditions.

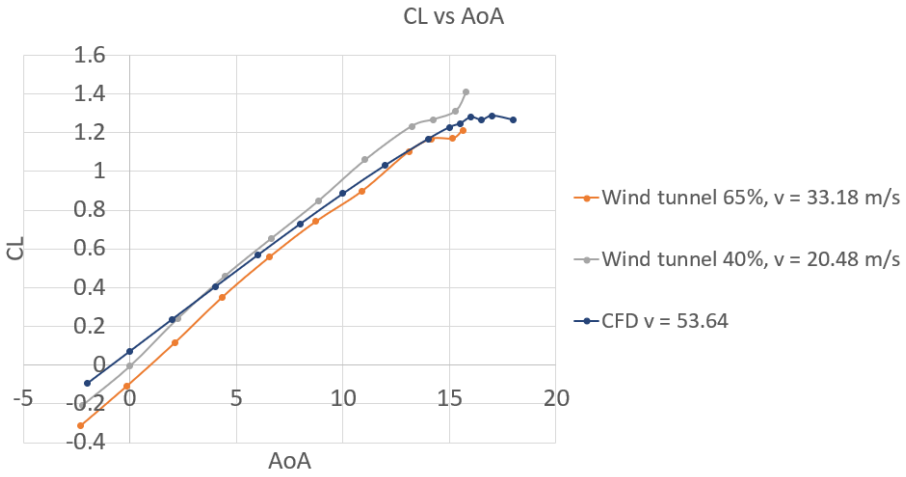

Figure 7 – Validation of CFD results with experimental data.

4. Results

A CFD analysis has been conducted for all the thirty DoE cases. Results have been evaluated in terms of lift-to-drag ratio (C_L/C_D) at an angle of attack (AoA) of 15.5° and compared to the baseline values. Even though it is well known that tubercles have the most positive effects in the post-stall regimes (Sec.1), the result analysis presented in this section is focused right before the stall happens. The reason of that is linked to the choice of considering steady CFD simulations. Unfortunately, the steady state option is not suitable for capturing transient phenomena that characterize the flow at post-stall regimes; therefore beyond an AoA of 15.5°, the residuals and the C_L/C_D of the tubercle cases show a very strong fluctuating behavior (Fig.10) leading to an unreliability of the results. Transient simulations will be considered for future publications. In the present work, the steady CFD analysis has been limited to the AoA where the steady option can be considered reliable.

As just mentioned, most of the DoE cases did not reach a convergence in the results (Fig.11), but the ones with reliable results show a relevant increase in C_L/C_D compared to the baseline wing. The converging results are listed in Tab.3 and plotted in Fig.12, where Fig.12a highlights the comparison with the baseline wing, and Fig.12b zooms in to show in detail the values of the lift-to-drag ratio of the considered tubercle cases.

Unfortunately, the area in the design space where tubercles positively affect the wing performance is not well defined (Fig.11). The reason of that is probably due to the simplified choice of steady CFD simulations. Therefore, a more detailed exploration of the design space is necessary and it will be

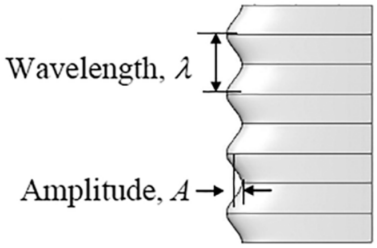

Figure 8 – Tubercles amplitude and wavelength.[11]

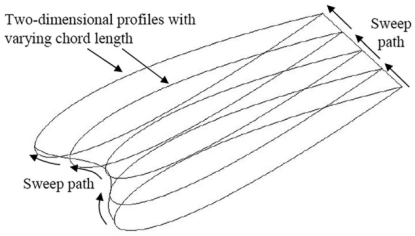

Figure 9 – Tubercles representation.[11]

conducted in future works.
Figure 13 represents the seven tubercle configurations that show positive results. As it is possible to notice, tubercles cover only the second mid-span of the wing in most of the represented cases. This means that they are characterized by low values of amplitude and moderate values of wavelength. These tubercle shapes look very "soft" and they result to have the most relevant lift-to-drag ratio improvement with respect to the baseline. On the other hand, only two (Tb7, Tb23) of the seven cases shown in Fig.13 are characterized by sharper tubercles, and they are also represented by the two lowest points in the plot in Fig.12b.
The reason of the lift-to-drag ratio improvement of these tubercle configurations compared to the baseline wing is probably linked to the generation of counter-rotating vortices that start from the tubercle peaks and move to the throats. Figure 14b highlights these vortices by showing the contour lines of the spanwise velocity plotted on a plane right behind tubercles. The same plane is used for the baseline results (Fig.14a) in order to compare them with the wing with tubercles.
As mentioned in Sec.1,.the counter-rotating vortices are able to block a portion of the spanwise flow that moves from the tip to the root of the wing. This is visible in Fig.15,16 where the spanwise velocity is plotted at the peak and throat sections of Tb10. Those results are also compared with the ones of the baseline at the same section locations. It is possible to notice how the strength of the spanwise velocity on the suction side of the wing with tubercles is lower compared to the one on the baseline wing at the same cross-section. This spanwise blockage also affects the lift and drag results of the

	C_L	C_D	C_L/C_D
Baseline	1.2471	0.1092	11.4118
Tb7	1.2461	0.0908	13.7139
Tb10	1.2512	0.0909	13.7524
Tb14	1.2500	0.0909	13.7441
Tb23	1.2473	0.0908	13.7298
Tb24	1.2510	0.0911	13.7318
Tb28	1.2480	0.0907	13.7452
Tb29	1.2515	0.0910	13.7467

Table 3 – Results for AoA = 15.5°.

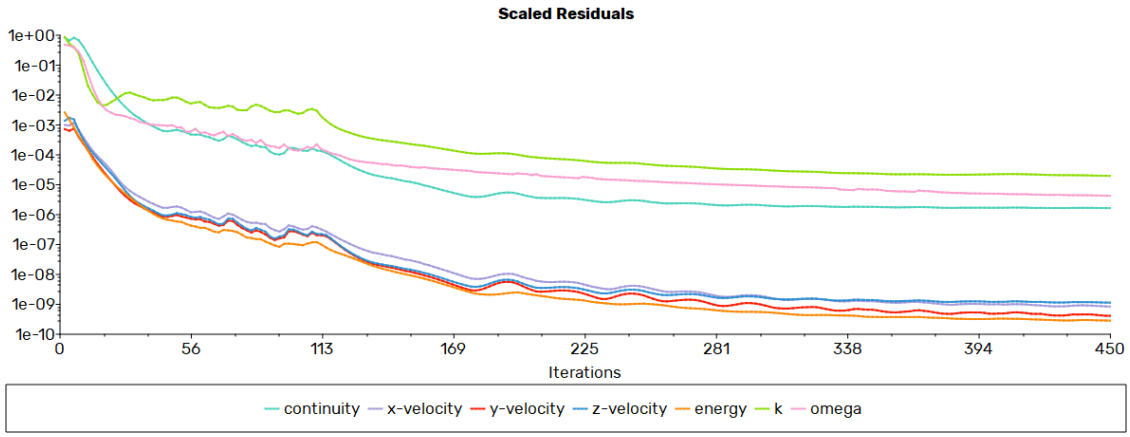

(a) AoA = 15.5°

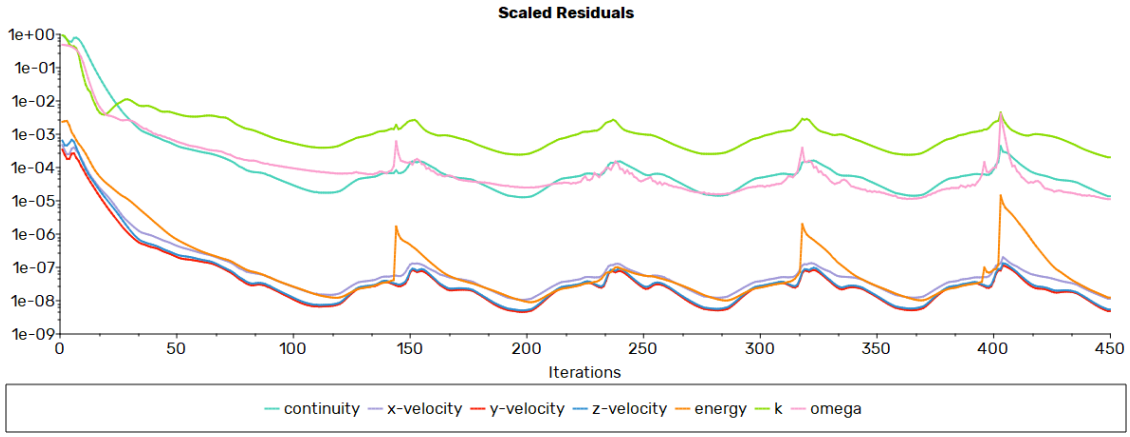

(b) AoA = 16°

Figure 10 – CFD residuals for the baseline wing.

wing with tubercles as shown in Tab.3.

5. Morphing Ideas

As mentioned before, the importance of tubercles in the aerodynamics of a wing is limited in the off-design regimes. The baseline wing is already optimally designed for the design conditions, therefore, a change in its shape – like a sinusoidal leading-edge – can be detrimental in terms of aerodynamics. Therefore, the idea is to design tubercles as morphing structures that "appears" on the wing leading-edge only when needed. The morphing concept behind them is still under investigation but some ideas considering smart materials and actuators are already in place and will be presented soon.
The results of this study show that very "soft" changes in the leading-edge shape and limited to the wing tip region are enough to achieve a relevant increase in the lift-to-drag ratio. From a structural point of view, this implies less stresses and strains to consider in the design phase of the possible morphing mechanism. However, a particular attention must go to the limits and tolerances of the stretchable materials available for such applications.

6. Conclusion

The work presented in this paper wants to give some insights on the characteristics of tubercles (amplitude, wavelength, and span-coverage) applied to the leading-edge of the Cessna 172 Skyhawk wing. The goal is to improve the aerodynamic performance during off-design flight regimes.
A design of experiment with three design variables (amplitude, wavelength, and number of tubercle peaks) has been considered for the design space exploration and in order to define the tubercle configuration to analyze. Thirty cases have been aerodynamically simulated but only seven of them

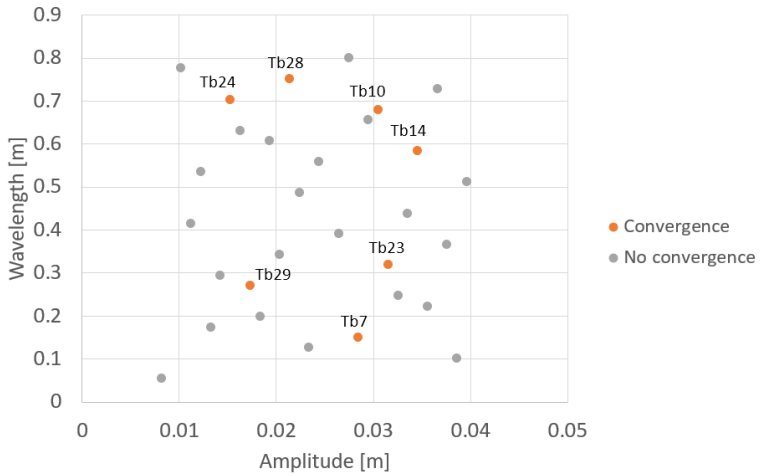

Figure 11 – DoE tubercle cases.

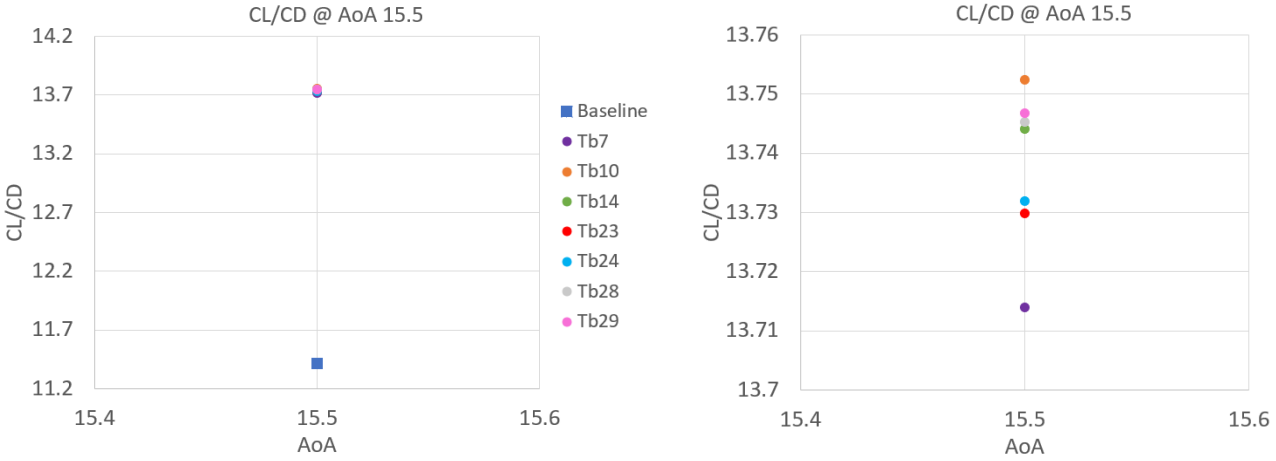

(a) Baseline vs tubercles

(b) Tubercle cases

Figure 12 – C_L/C_D at AoA = 15.5°.

showed convergence results. The main reason of that is in the choice of steady CFD analysis in order to reduce the computational costs for this preliminary study. However, those seven tubercle configurations showed a relevant improvement in the lift-to-drag ratio with respect to the baseline when the flow is characterized by a high angle of attack (15.5°). Such a performance enhancement is due to the effect that the counter-rotating vortices generated at the tubercle peaks have on the spanwise flow. They create a blockage effect leading to an increase in lift and reduction in drag. Moreover, the concept explored in the present study also wants to consider the possibility of making such tubercles morphing. Since their major effects are visible at off-design regimes, smart materials and actuators can enable the change in shape of the baseline wing leading-edge into tubercles only when needed. It has been observed that small values of amplitudes, and few tubercles placed close to the wing tip result to have promising results in terms of lift-to-drag ratio; therefore, such "soft" tubercle shapes might be easily transformed into morphing structures.
More studies on the effects of tubercles on wings will be conducted in future works with a particular attention on a better exploration of the design space, and on a structural design of morphing tubercles.

7. Copyright Statement

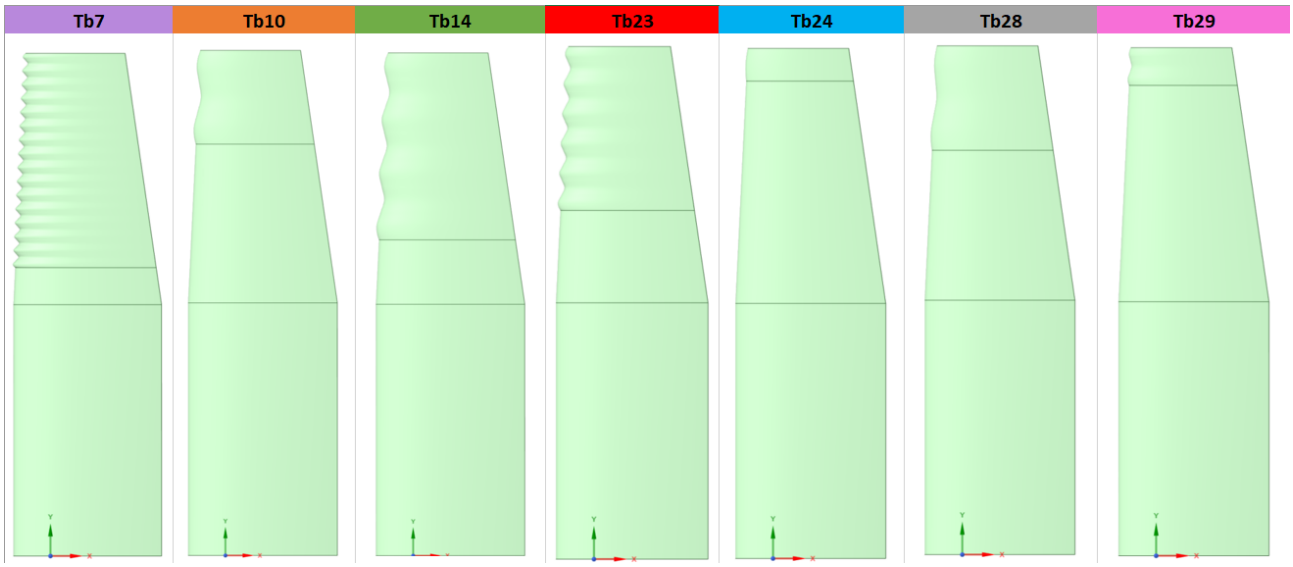

Figure 13 – Tubercle shapes of wings with convergent results.

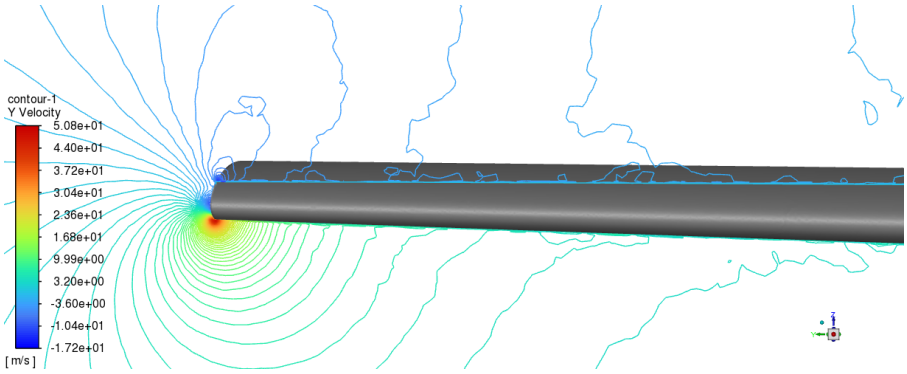

(a) Baseline

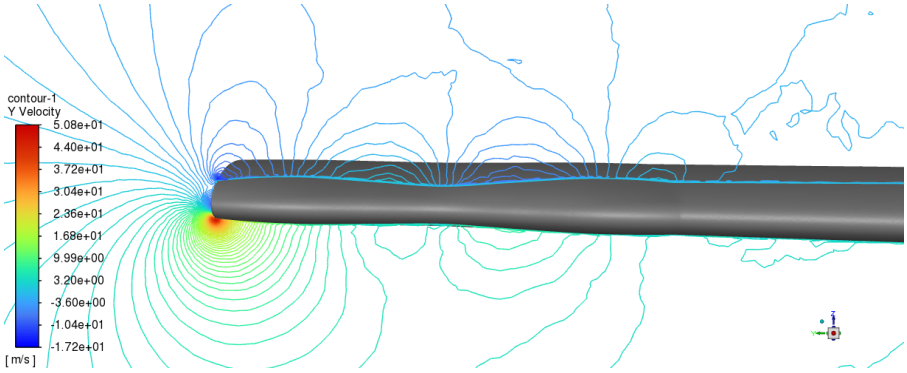

(b) Tb10

Figure 14 – Contour spanwise velocity lines for baseline and Tb10.

(a) Baseline

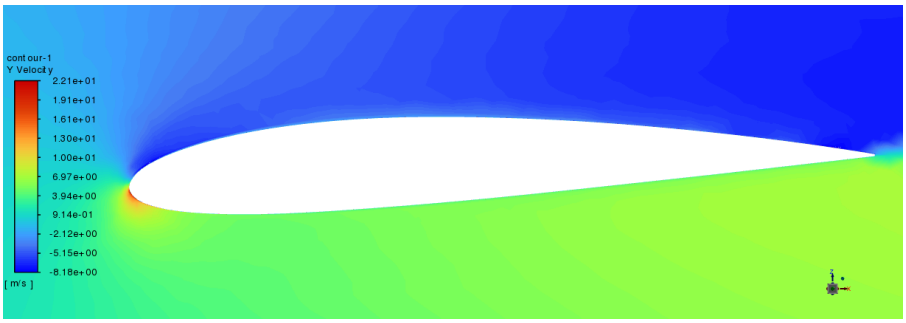

(b) Tb10

Figure 15 – Contour spanwise velocity plot for baseline and Tb10 at a peak section.

(a) Baseline

(b) Tb10

Figure 16 – Contour spanwise velocity plot for baseline and Tb10 at a throat section.

holder of this paper, for the publication and distribution of this paper as part of the ICAS proceedings or as individual off-prints from the proceedings.

References

[1] Franke E. Fish and Juliann M. Battle. Hydrodynamic design of the humpback whale flipper. *Journal of morphology*, 225(1):51–60, 1995.

[2] F.E. Fish and G.V. Lauder. Passive and active flow control by swimming fishes and mammals. *Annu. Rev. Fluid Mech.*, 38:193–224, 2006.

[3] D.S. Miklosovic, M.M. Murray, L.E. Howle, and F.E. Fish. Leading-edge tubercles delay stall on humpback whale (megaptera novaeangliae) flippers. *Physics of fluids*, 16(5):L39–L42, 2004.

[4] Kristy L. Hansen, Richard M. Kelso, and Bassam B. Dally. Performance variations of leading-edge tubercles for distinct airfoil profiles. *AIAA journal*, 49(1):185–194, 2011.

[5] Kristy Lee Hansen. *Effect of leading edge tubercles on airfoil performance.* PhD thesis, 2012.

[6] Kristy L. Hansen, Nikan Rostamzadeh, Richard M. Kelso, and Bassam B. Dally. Evolution of the streamwise vortices generated between leading edge tubercles. *Journal of Fluid Mechanics*, 788:730–766, 2016.

[7] Ri-Kui Zhang and Van Dam Jie-Zhi Wu. Aerodynamic characteristics of wind turbine blades with a sinusoidal leading edge. *Wind Energy*, 15(3):407–424, 2012.

[8] Giada Abate and Dimitri N. Mavris. Cfd analysis of leading edge tubercle effects on wind turbine performance. In *15th international energy conversion engineering conference*, page 4626, 2017.

[9] Giada Abate and Dimitri N. Mavris. Performance analysis of different positions of leading edge tubercles on a wind turbine blade. In *2018 Wind energy symposium*, page 1494, 2018.

[10] Giada Abate, Dimitri N. Mavris, and Lakshmi N. Sankar. Performance effects of leading edge tubercles on the nrel phase vi wind turbine blade. *Journal of Energy Resources Technology*, 141(5):051206, 2019.

[11] Giada Abate. A numerical investigation into the aerodynamic effects of tubercles in wind turbine blades. *PhD diss., Georgia Institute of Technology*, 2019.

[12] L.L.C. Bellequant and Laurens E. Howle. Whalepower wenvor blade. 2009.

[13] Giorgio Moscato, Jais Mohamed, and Giovanni Paolo Romano. Improving performances of biomimetic wings with leading-edge tubercles. *Experiments in Fluids*, 63(9):146, 2022.

[14] Aleyna Çolak, Mehmet Seyhan, and Mustafa Sarioğlu. Leading-edge tubercle modifications to the biomimetic wings. *Physics of Fluids*, 35(1), 2023.

[15] Hamid Johari, Charles Henoch, Derrick Custodio, and Alexandra Levshin. Effects of leading-edge protuberances on airfoil performance. *AIAA journal*, 45(11):2634–2642, 2007.

[16] Alex Skillen, Alistair Revell, Alfredo Pinelli, Ugo Piomelli, and Julien Favier. Flow over a wing with leading-edge undulations. *Aiaa Journal*, 53(2):464–472, 2015.

[17] S.M.A. Aftab, N.A. Razak, A.S. Mohd Rafie, and K.A. Ahmad. Mimicking the humpback whale: An aerodynamic perspective. *Progress in Aerospace Sciences*, 84:48–69, 2016.

[18] S.M.A. Aftab and K.A. Ahmad. Cfd study on naca 4415 airfoil implementing spherical and sinusoidal tubercle leading edge. *PloS one*, 12(8):e0183456, 2017.

[19] Ming Zhao, Tong Wei, Yijia Zhao, and Zhengxian Liu. Influences of leading-edge tubercle amplitude on airfoil flow field. *Journal of Thermal Science*, 32(4):1335–1344, 2023.

[20] C. Cai, Z.G. Zuo, S.H. Liu, Y.L. Wu, and F.B. Wang. Numerical evaluations of the effect of leading-edge protuberances on the static and dynamic stall characteristics of an airfoil. In *IOP Conference Series: Materials Science and Engineering*, volume 52, page 052006. IOP Publishing, 2013.

[21] Adson A. de Paula, Julio Meneghini, Vitor Gabriel Kleine, and Roberto D. Girardi. The wavy leading edge performance for a very thick airfoil. In *55th AIAA Aerospace Sciences Meeting*, page 0492, 2017.

[22] A. Dropkin, D. Custodio, C.W. Henoch, and H. Johari. Computation of flow field around an airfoil with leading-edge protuberances. *Journal of Aircraft*, 49(5):1345–1355, 2012.

[23] Amirfarhang Nikkhoo and Ali Esmaeili. Numerical study of geometrical properties of full-span tubercle leading edge wing at post-stall condition. *Journal of Applied Fluid Mechanics*, 16(9):1752–1766, 2023.

[24] M.D. Bolzon, R.M. Kelso, and M. Arjomandi. The effects of tubercles on swept wing performance at low angles of attack. In *Proceedings of the 19th Australasian fluid mechanics conference*, pages 8–11. Australasian Fluid Mechanics Soc. Melbourne, Australia, 2014.

[25] Zhaoyu Wei, Tze How New, and YD Cui. Aerodynamic performance and surface flow structures of leading-edge tubercled tapered swept-back wings. *AIAA Journal*, 56(1):423–431, 2018.

[26] Veerapathiran Thangaraj Gopinathan, John Bruce Ralphin Rose, and Mohanram Surya. Investigation on

the effect of leading edge tubercles of sweptback wing at low reynolds number. *Mechanics & Industry*, 21(6):621, 2020.

[27] Adson A. de Paula, Alejandro A. Rios Cruz, Paulo H. Ferreira, Vitor G. Kleine, and Roberto G. da Silva. Swept wing effects on wavy leading edge phenomena. In *2018 Flow Control Conference*, page 4253, 2018.

[28] Charalampos Papadopoulos, Vasilis Katsiadramis, and Kyros Yakinthos. Numerical 3d study on the influence of spanwise distribution of tubercles on wings for uav applications. In *MATEC Web of Conferences*, volume 304, page 02014. EDP Sciences, 2019.

[29] biomimicry2016. https://biomimicry2016.wordpress.com/, 2016.

[30] Naseer A. Mousa, Osam H. Attia, Hussein A. Mahmood, and Nor Mariah Adam. Optimization efficiency of the aircraft wing of cessna 172 skyhawk by absorbent adverse pressure using tangential suction slot without vacuum device. *Mathematical Modelling of Engineering Problems*, 9(3), 2022.

[31] Sergiu Petre Iliev and Vito L. Tagarielli. Cessna 172 wind tunnel test. *Imperial College - Department of Aeronautics, London*, 2013.

[32] Tey Jia Sheng. Wind tunnel test on model cessna. *Imperial College - Department of Aeronautics, South Kensington Campus*, 2018.